Biophysical Journal, Volume *114*

Supplemental Information

Membrane Bending Moduli of Coexisting Liquid Phases Containing Transmembrane Peptide

Rebecca D. Usery, Thais A. Enoki, Sanjula P. Wickramasinghe, V.P. Nguyen, David G. Ackerman, Denise V. Greathouse, Roger E. Koeppe, Francisco N. Barrera, and Gerald W. Feigenson

Supporting Material

Bending modulus measurement- additional information

Bending modulus measurements were carried out with fluctuation analysis as in (1) implemented in Matlab version 2014b.

To ensure the harvested GUVs were slightly flaccid for fluctuation analysis, an osmolality difference between the sucrose and glucose solutions of 4 - 5 mOsmol/kg H_2O was ensured with the use of an osmometer (Model 5004, Precision Systems Inc., Natick, MA). GUVs were formed in 97 mM sucrose solution and harvested into 101 mM glucose solution. Due to the density difference and potential distortion by gravity, we limited the size of vesicles to those having radii less than 20 μm (2).

Sample chambers for observation consisted of a no. 1.5 coverslip and traditional microscope slide separated with a silicone spacer (Sigma-Aldrich, St. Louis, MO) of 0.25 mm thickness. All observations took place at room temperature of ~ 23°C. 0.02 mol% C12:0 DiI was included in GUV preparations and fluorescence intensity was used to exclude any vesicles having more than one bilayer (3).

Datasets consisted of 1600 1 ms exposures. Contours were defined using Canny edge detection with $\sigma = 2$ in images with a pixel size of 79 nm. To ensure the contours were approximately circular the ratio of enclosed area to total perimeter is compared to the approximate radius in each frame. We excluded frames in which the contour reflected a change in radii greater than 10% compared to previous frames.

Compositions for Bending Measurements

In Fig. S1, the compositions for each of the four ternary mixtures used in this study are depicted on diagrams with their respective two-phase regions as defined by previous work (4, 5).

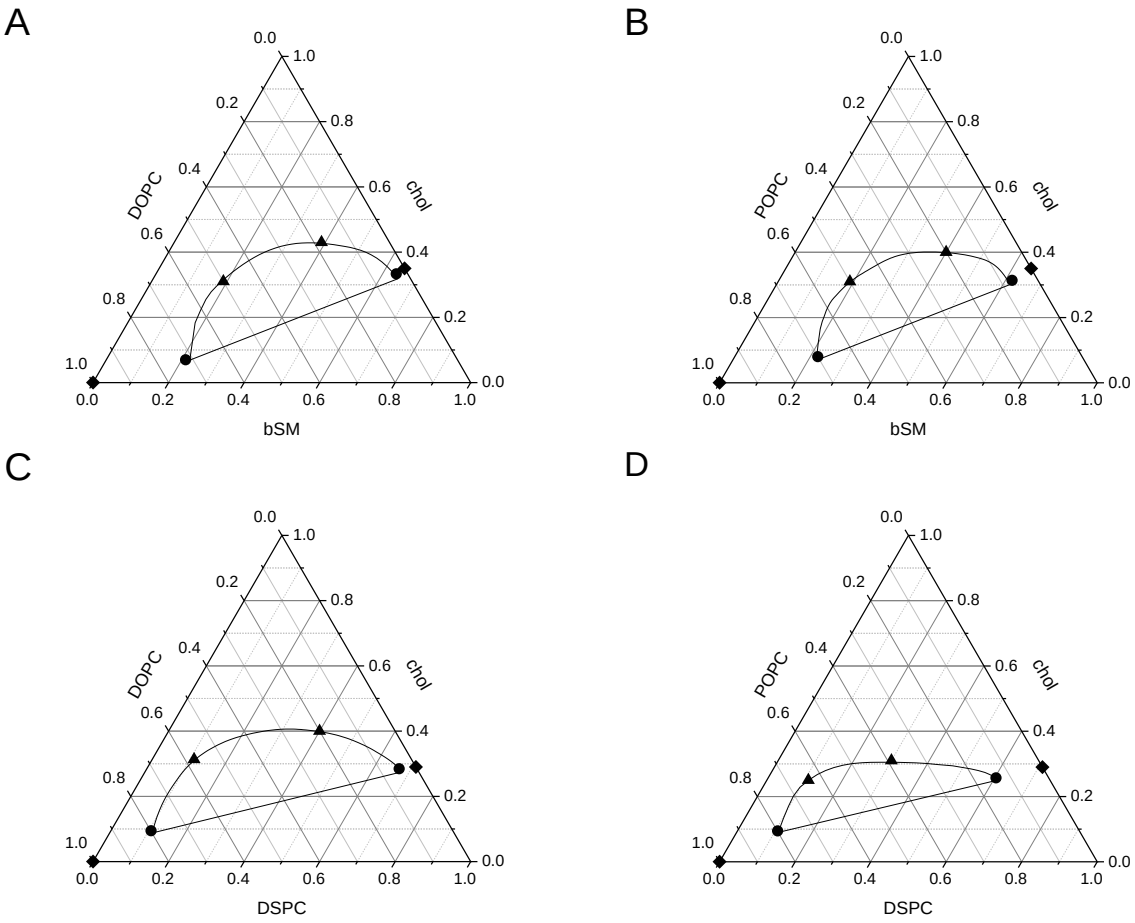

FIGURE S1 Compositions used for bending moduli measurements. The ternary mixtures examined in this work include bSM/DOPC/chol (A), bSM/POPC/chol (B), DSPC/DOPC/chol (C), and DSPC/POPC/chol (D). For each, the simplified (♦), lower tieline endpoint (●), and high cholesterol tieline endpoint (▲) compositions are shown.

Parameters for FRET measurements

FRET along compositional trajectories was used to determine phase boundaries as previously described (6, 5, 4). Partition coefficients were also determined by these means and fitting the experimental data was done as described in the main text. In the FRET experiments, the fluorescence of each dye individually is monitored. The excitation and emission wavelengths for the probes used in this study are detailed in Table S1. The FRET pairs used in this work and corresponding emission and excitation wavelengths monitored are described in Table S2.

Probe	λ_{ex}	λ_{em}
Trp	284	335
DHE	327	393
FAST DiO	477	503
BODIPY-PC	500	520

TABLE S1 Emission (λ_{ex}) and excitation (λ_{em}) wavelengths for individual dye fluorescence.

Donor	**Acceptor**	λ_{ex}	λ_{em}
Trp	DHE	284	393
Trp	BODIPY-PC	284	520
DHE	FAST DiO	327	503
DHE	BODIPY-PC	327	520

TABLE S2 Emission (λ_{ex}) and excitation (λ_{em}) wavelengths for FRET pairs used in this study.

GWALP23 K_p in nanoscopic mixtures

We prepared sample trajectories parallel to the lower tieline for the nanoscopic mixtures, DSPC/POPC/chol and bSM/POPC/chol. FRET from GWALP23 tryptophan to BODIPY-PC is shown in Fig. S2. Though the best fit solid lines indicate K_p of the peptide is 4 ± 1 and 3 ± 1 in DSPC/POPC/chol and bSM/POPC/chol, respectively, the actual preference of the peptide for Ld would be larger than this fitting suggests because domain size is near the magnitude of the Förster Radius, Ro.

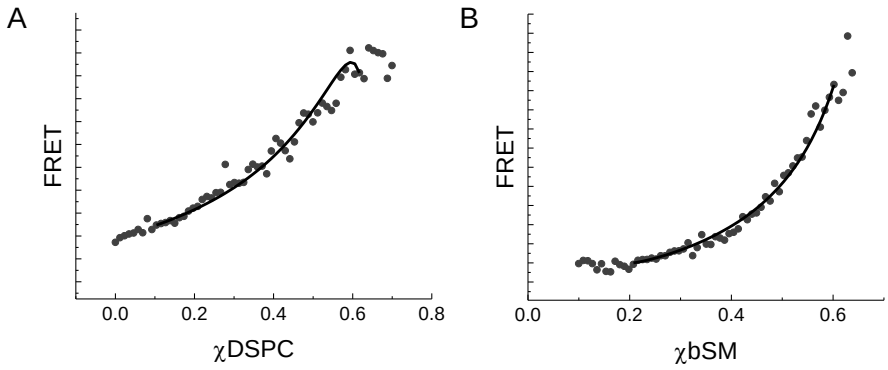

FIGURE S2 GWALP23 partitions into the Ld phase of mixtures with coexisting nanoscopic Ld + Lo domains. (A) FRET (solid circles, AU) from the GWALP23 tryptophan to BODIPY-PC is plotted with respect to DSPC fraction along the trajectory for DSPC/POPC/chol shown in Fig. 1A. The best fit (solid line) to Eq. 2 yields $K_p = 4 \pm 1$. (B) FRET (solid circles, AU) from the GWALP23 tryptophan to BODIPY-PC is plotted with respect to bSM fraction along a trajectory parallel to the lower tieline of the two-phase region for bSM/POPC/chol (4) analogous to that shown in Fig. 1A. The best fit (solid line) to Eq. 2 yields $K_p = 3 \pm 1$. Trajectories included 0.5 mol% GWALP23.

C12:0 DiI Fluorescence calibration

GUV preparations included 0.1 mol% C12:0 DiI. The sample size was varied and lipid concentration was determined by phosphate assay (7). We collected the fluorescence of C12:0 DiI (547/565 ex/em) for these samples. As anticipated, the steady state fluorescence of C12:0 DiI included at a fixed fraction is directly proportional to the lipid concentration, Fig. S3. Thus, the ratio of GWALP23 Trp fluorescence to C12:0 DiI fluorescence is indicative of the protein:lipid ratio in GUV preparations.

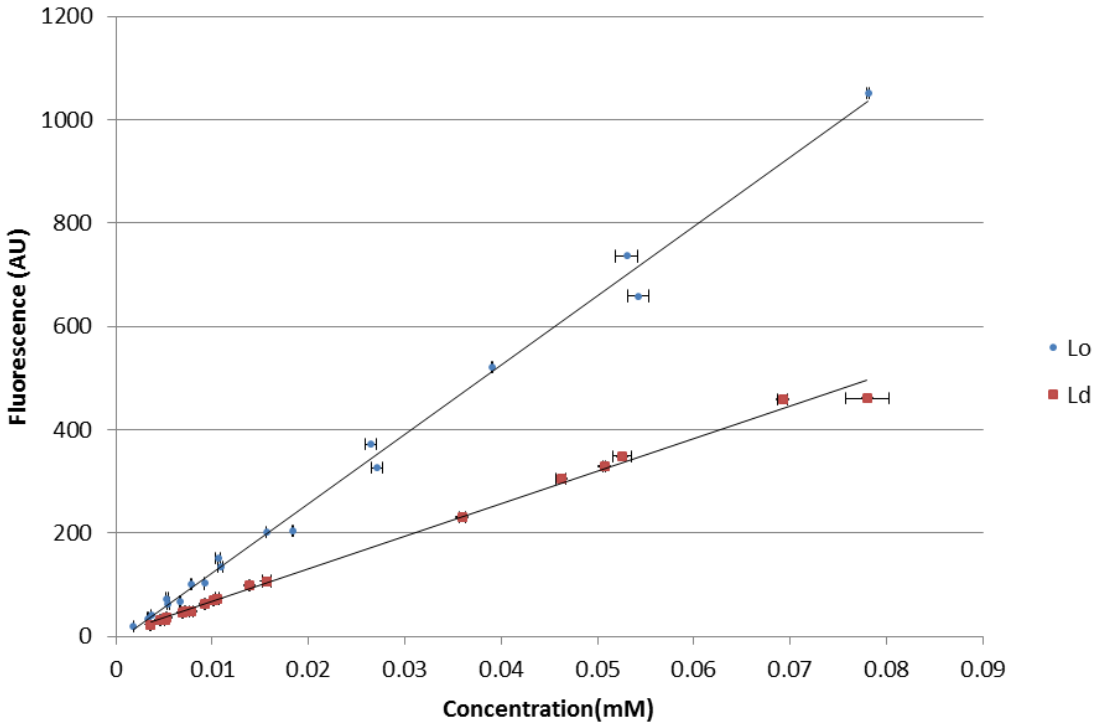

FIGURE S3 C12:0 DiI fluorescence is directly proportional to the lipid concentration. C12:0 DiI fluorescence in Ld (red squares) and Lo (blue circles) is plotted with respect to lipid concentration.

EPR experiments

In an effort to understand how GWALP23 affects membrane lipids, we also conducted EPR experiments using 7PC and 16PC probes. EPR spectra are shown in Fig. S4, and the data is summarized in Table S3. We find the peptide did not significantly affect order along the acyl chains in DSPC/DOPC/chol for Ld. the order and the rate of motion of the acyl chains in Ld did not change in the presence of up to 4 mol% GWALP23. This implies that the significant increase in the bending modulus was not caused by a significant change in the material properties of each leaflet of Ld.

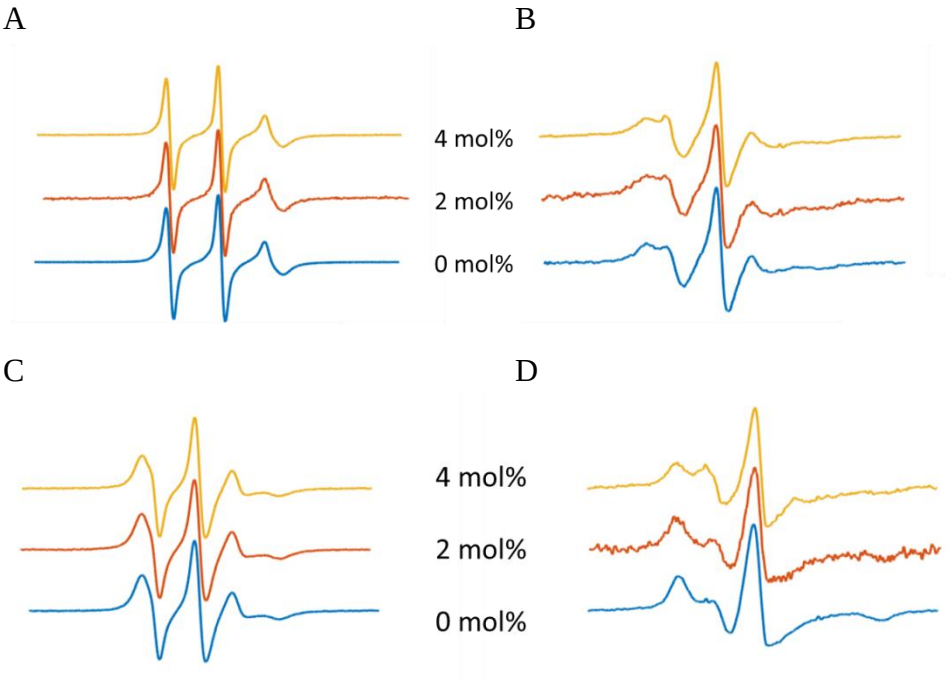

FIGURE S4 EPR spectra for Ld (A, B) and Lo (C, D) with 16:0-16 Doxyl PC (A, C) and 16:0-7Doxyl PC (B, D) with 0 (blue), 2 (orange), and 4 (yellow) mol% WALP23.

spin label	GWALP23 (mol%)	S_{Ld}	S_{Lo}
16 Doxyl PC	0	0.13	0.33
	2	0.12	
	4	0.13	
7 Doxyl PC	0	0.29	0.41
	2	0.28	
	4	0.29	

TABLE S3. DSPC/DOPC/chol Ld and Lo order parameters (S_{Ld} and S_{Lo}, respectively) with 0, 2, and 4 mol% GWALP23. Order parameter for Lo with GWALP23 not depicted based on OCD experiments.

Partitioning of FAST DiO at high- and low-cholesterol

For the mixture DSPC/DOPC/chol, we determined the partition coefficient of FAST DiO between Ld and Lo at low and high cholesterol content. The K_p of FAST DiO is 12 ± 2 at low cholesterol content and 4 ± 1 at high cholesterol content, Fig. S5. This change in K_p mirrors the change in K_p observed for GWALP23, Figs 2A and 7.

A B

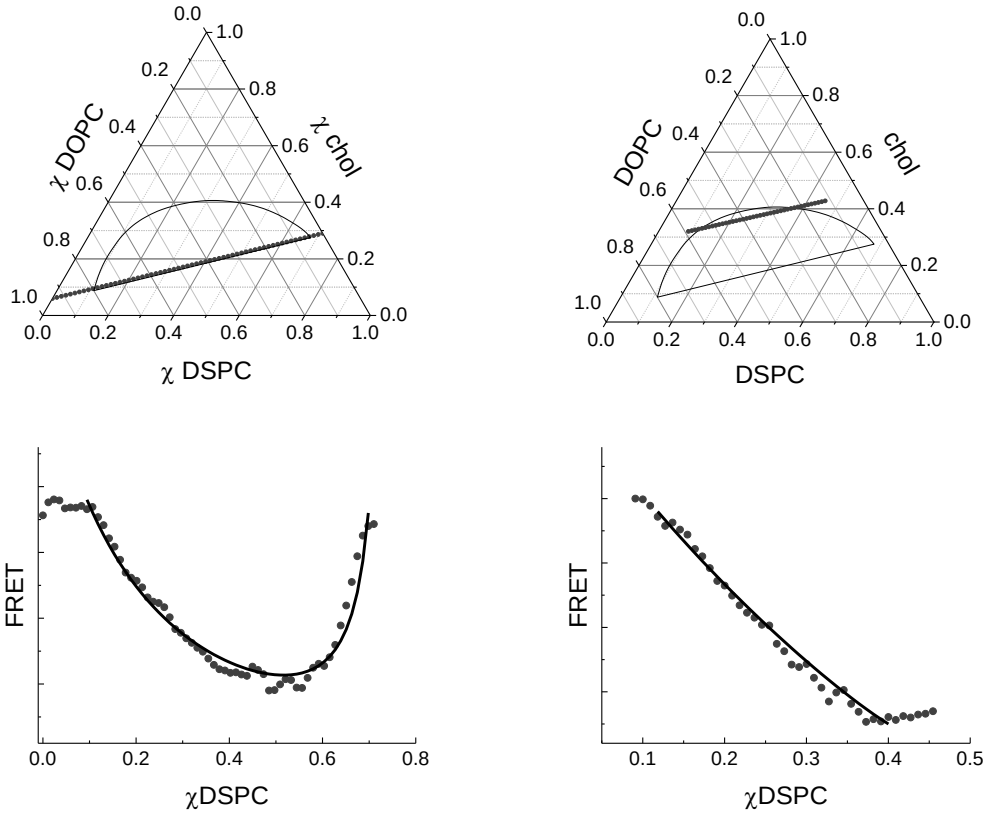

FIGURE S5 FAST DiO K_p decreases with increased cholesterol content. (A) Diagram showing the sample compositions used in low-cholesterol trajectory coinciding with the lower tieline of the two-phase region. Intensity of FRET from DHE to FAST DiO along the trajectory is shown in the lower panel. The best fit of the experimental data (solid line) yields K_p = 12 ± 2. (B) Diagram illustrating the compositional space traversed by the high-cholesterol trajectory and the phase coexistence region (Ld+Lo) for DSPC/DOPC/chol. Lower panel shows the intensity of FRET from DHE to FAST DiO. The best fit of the experimental data (solid line) yields K_p = 4 ± 1.

Bending modulus of DOPC + GWALP23

For comparison to the ternary mixtures, we measured the bending modulus of a simplified Ld phase, DOPC, with peptide. Like the ternary Ld phases, the bending modulus increased with peptide concentration, but the increase was more gradual. For this simplified Ld phase, GUV yield could be maintained with a higher fraction of peptide.

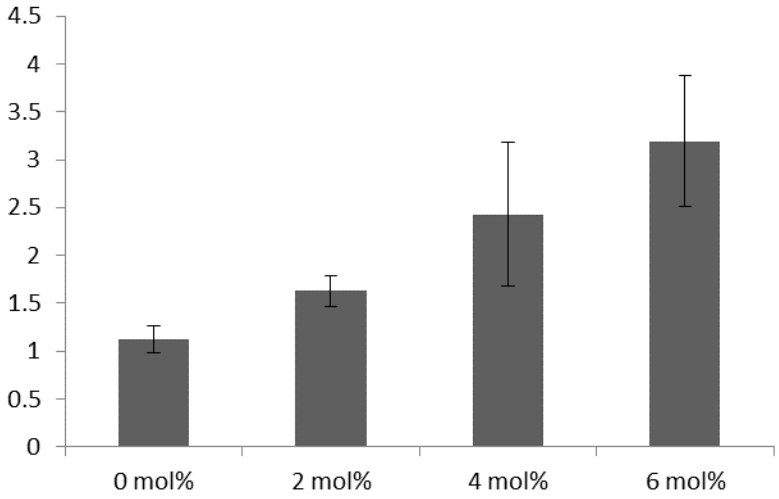

FIGURE S6 GWALP23 increases the membrane bending rigidity of the DOPC membranes. Bending moduli, κ, in 10^{-19} J of DOPC with 0, 2, 4, and 6 mol% GWALP23.

References

1. Usery, R.D., T.A. Enoki, S.P. Wickramasinghe, M.D. Weiner, W.-C. Tsai, M.B. Kim, S. Wang, T.L. Torng, D.G. Ackerman, F.A. Heberle, J. Katsaras, and G.W. Feigenson. 2017. Line Tension Controls Liquid-Disordered + Liquid-Ordered Domain Size Transition in Lipid Bilayers. Biophys. J. 112: 1431–1443.

2. Henriksen, J.R., and J.H. Ipsen. 2002. Thermal undulations of quasi-spherical vesicles stabilized by gravity. Eur. Phys. J. E. Soft Matter. 9: 365–74.

3. Akashi, K., H. Miyata, H. Itoh, and K. Kinosita. 1996. Preparation of giant liposomes in physiological conditions and their characterization under an optical microscope. Biophys. J. 71: 3242–50.

4. Petruzielo, R.S., F.A. Heberle, P. Drazba, J. Katsaras, and G.W. Feigenson. 2013. Phase behavior and domain size in sphingomyelin-containing lipid bilayers. Biochim. Biophys. Acta. 1828: 1302–13.

5. Konyakhina, T.M., J. Wu, J.D. Mastroianni, F.A. Heberle, and G.W. Feigenson. 2013. Phase diagram of a 4-component lipid mixture: DSPC/DOPC/POPC/chol. Biochim. Biophys. Acta. 1828: 2204–14.

6. Zhao, J., J. Wu, F. a Heberle, T.T. Mills, P. Klawitter, G. Huang, G. Costanza, and G.W. Feigenson. 2007. Phase studies of model biomembranes: complex behavior of DSPC/DOPC/cholesterol. Biochim. Biophys. Acta. 1768: 2764–76.

7. Kingsley, P. B., Feigenson, G.W. 1979. The Synthesis of a Perdueterated Phospholipid: 1,2-dimyristoyl-sn-glycero-3-phosphocholine-d72. Chem. Phys. Lipids. 24: 135–147.